Malaysian Journal of Analytical Sciences (MJAS)
Published by Malaysian Analytical Sciences Society

PHYSICOCHEMICAL STUDY ON ALKOXYLATED AZO-IMINE CHITOSAN-BASED BIOPOLYMER FOR ELECTROLYTE APPLICATIONS

(Kajian Fizikokimia ke atas Biopolimer Alkoksi Azo-Imina Berasaskan Kitosan bagi Aplikasi Elektrolit)

Tuan Siti Fatimah Tuan Mohd Pauzi[1], Rafizah Rahamathullah[1*], M. N. Hafiza[2], Wan M. Khairul[3]

[1]*Faculty of Chemical Engineering & Technology, Universiti Malaysia Perlis, 02600 Arau, Perlis, Malaysia*
[2]*Faculty of Maritime Studies, Universiti Malaysia Terengganu, 21030, Kuala Nerus, Terengganu, Malaysia*
[3]*Faculty of Science and Marine Environment, Universiti Malaysia Terengganu, 21030, Kuala Nerus, Terengganu, Malaysia*

[*]*Corresponding author: fizah@unimap.edu.my*

Received: 15 September 2023; Accepted: 25 February 2024; Published: 29 April 2024

Abstract

The performance of electrolytes in electronic applications are in decline due to low ionic conductivity, leakage, and inadequate thermal stability. Overcoming these challenges necessitates innovative approaches which includes electrolyte design, and materials selection, that should be taken into consideration. In this study, new additive alkoxylated azo-imine (**AZ**) material containing hybrid moieties of azo (-N=N-) and imine (-CH=N-) groups was successfully synthesized, characterized, and doped in biopolymer matrix. Chitosan-based biopolymer was formulated with **AZ** additive material as solid biopolymer electrolyte (SBE) through the concept of Donor (D) - π- Acceptor (A). The prepared **AZ** additive was characterized by selected spectroscopic and thermal analyses using FTIR, 1D NMR, and TGA before integration as SBE. The thermogram of **AZ** additive revealed good thermal stability up to 300 °C, making it suitable for application as electrolytes. Several weight percentages (2%-8%) of additive were doped with chitosan biopolymer as new SBEs (**F1-F4**). The conductivity of prepared SBE was measured via electrochemical impedance spectroscopy (EIS) which achieved the highest ionic conductivity of 8.22 x 10^{-3} S cm^{-1} at room temperature (303K). The preliminary findings suggest that this organic material has significant potential as an additive material in electrolyte application.

Keywords: additive, azo-imine, biopolymer electrolyte, conductivity, chitosan

Abstrak

Prestasi elektrolit dalam aplikasi elektronik semakin merosot kerana konduktiviti ion yang rendah, kebocoran, dan ketidakstabilan terma. Bagi mengatasi cabaran ini, pendekatan inovatif termasuk reka bentuk elektrolit dan pemilihan bahan perlu diberi perhatian. Dalam kajian ini, bahan tambah baharu azo-imina alkoksi (**AZ**) yang mengandungi moieti campuran azo (-N=N-) dan imina (-CH=N-) telah berjaya disintesis, dicirikan, dan dicampurkan ke dalam matriks biopolimer. Biopolimer berasaskan kitosan telah diformulasikan dengan bahan tambah **AZ** sebagai elektrolit pepejal biopolimer (SBE) melalui konsep Penderma (D) - π - Penerima (A). Bahan tambah **AZ** yang disediakan telah dicirikan menggunakan analisis spektroskopi dan terma yang terpilih menggunakan FTIR, 1D NMR, dan TGA sebelum digabungkan sebagai SBE. Termogram bahan tambah **AZ** menunjukkan kestabilan terma yang baik sehingga 300 °C, menjadikannya sesuai untuk digunakan sebagai elektrolit. Beberapa peratusan berat (2-8 wt. %) bahan

tambah telah dicampurkan dengan biopolimer kitosan sebagai SBE baharu (**F1-F4**). Kekonduksian SBE yang sediakan telah diukur melalui spekstroskopi impedans elektrokimia (EIS) dan mencapai konduktiviti 8.22 x 10^{-3} S cm^{-1} pada suhu bilik (303 K). Keputusan awal menunjukkan bahawa bahan organik ini mempunyai potensi yang baik sebagai bahan tambah dalam aplikasi elektrolit.

Kata kunci: bahan tambah, azo-imina, biopolimer elektrolit, kekonduksian, kitosan

Introduction

Electrolytes are a crucial component in energy storage devices, and these includes capacitors, batteries, and fuel cells [1]. The properties of the electrolyte, such as potential window, resistivity, conductivity, viscosity, stability, and flexibility, provides a huge impact on device performance [2]. A wide variety of electrolytes have been explored, including liquid electrolytes (aqueous, organic, and ionic liquid) [3] and solid-state electrolytes [4] as the potential ideal electrolyte. In this context, there is a high demand on liquid electrolytes-based alkali metals, lithium salts and organic solvent due to their performance in high ionic conductivity, capability to form stable contact with electrode, and the ability to reach high-rate performance in devices [5, 6]. Despite its superior performance, electrolytes have their own set of shortcomings as they are susceptible to corrosion and leakage issues, leading to device degradation and the possibility of self-discharge to electronic waste (e-waste) [7]. To mitigate the risks associated with liquid electrolytes and harmful material, solid-state electrolytes have been considered as a promising alternative.

Solid-state electrolytes offer various advantages properties including non-flammable, no flowing and corrosion after damage, and higher operation temperature [8]. The development of sustainable and eco-friendly materials for electrolyte applications has initiated a growing demand for new materials that can enhance performance. Thus, biopolymers have emerged as a promising candidate for polymer matrix due to their abundant availability, biodegradability, and excellent physicochemical properties [9]. Specifically, the preceding research employed biopolymers such as cellulose, alginate, and starch as solid-state electrolytes with the conductivity of these biopolymers is in the magnitude range of 10^{-5} - 10^{-10} S cm^{-1} [1, 10, 11]. Among various biopolymers materials, chitosan has garnered considerable interest in biopolymer-based electrolytes, primarily because of its unique characteristics including high mechanical strength, good thermal stability, and excellent film-forming ability [12]. Nonetheless, its ionic conductivity is often restricted, posing a challenge for its optimal use in high-performance applications [13].

In this context, researchers focus on effective methods to boost up the ionic conductivity of electrolytes by incorporating small portion of additives into the biopolymer matrix [14]. Some of the strategies to achieve an ideal ionic conductivity of at least 10^{-3} S/cm in electrochemical application includes utilizing ionic liquids [15], increasing the amounts of inorganic salts [16], and incorporate the organic liquid plasticizers [17] into biopolymer. Nevertheless, plasticization can result in deterioration of the mechanical integrity of the film and increased corrosive reactivity of polymer electrolyte as it requires large amounts of plasticizers [18]. Recently, the functional additives containing nitrogen (N), oxygen (O), carbon (C), and hydrogen (H) have been extensively explored to enhance the ionic conductivity of biopolymer electrolytes which consequently improve the electrolyte performance [19, 20]. Hence, this study aims to prepare new organic functional additives for polymer-based electrolyte application. The new hybrid moiety of azo (-N=N-) and imino (-C=N-) with alkoxy chain has been tested to act as an additive in the attempts to explore their suitability in chitosan biopolymer matrix. Individually, the moiety of (-N=N-) and (-C=N-) have soft and hard donor functionalities, offer π-system that highly desirable for various applications in electrolyte [20, 21], optoelectronic [22], and sensor [23]. These conjugated π-systems provide electron delocalization and π-π stacking interactions, resulting in improved charged transport properties [24]. Thus, in this study, azo-imine additive has been incorporated with chitosan-based biopolymer and in turn, the performance is tested on electrolyte application. The combination of the mixed

soft-hard donor character and the intriguing properties of these compounds should open a new avenue for electrolyte application. The mixing of prepared **AZ** additive in biopolymer matrix system is expected to support the ion dissociation; and as a result, a greater number of migrating ions may become available for charge transport.

Materials and Instrumentations

The reagents, 4-nitroaniline, 4-acetamidophenol, 1-bromohexane, chitosan powder (high molecular weight (M_w), 310,000-375,000, salicylaldehyde, glacial acetic acid, potassium carbonate and ethanol were purchased from commercial suppliers. It was used without further purification. Fourier transform infrared (FTIR) spectroscopy was performed in the wavenumber range of 4000 – 400 cm^{-1} using the Bruker Invenio-S instrument via the Attenuated total reflectance (ATR) method. 1D Nuclear magnetic resonances (NMR) of ^{1}H and ^{13}C were conducted using the Varian NMR System 500 MHz instrument using tetramethylsilane (TMS) as internal standard in deuterated chloroform ($CDCl_3$). Thermogravimetric Analysis (TGA) was conducted using the Perkin Elmer analyzer, with a heating temperature ranging from 30 to 600 ℃ and a flowrate of 10 ℃/min under nitrogen atmosphere. The conductivity of the prepared SBE were run using electrical impedance spectroscopy (EIS) within the frequency range of 1 MHz to 50 Hz, employing the HIOKI 3532-50 LCR Hi-Tester.

Synthesis of alkoxylated azo-imine additive (AZ)

Prior to obtain **AZ** additive, azo salicylaldehyde (**1**), *N*-4-hexyloxy phenyl acetamide (**2a**) and *N*-4-hexyloxy aniline (**3a**) acting as precursors were attained via different designated reactions. The experimental details on the precursors (**1**, **2a** & **3a**) have been reported in previous studies [24–26]. Several modifications in term of synthetic pathway and characterization were carried out and are discussed further in this contribution. The precursor **1** was synthesized via diazotization process, using 4-nitroaniline (0.015 mole, 2g) and salicylaldehyde (0.015 mole, 1.8g). The progress of the compound's reaction completion was monitored using Thin Layer Chromatography (TLC) performed under ethyl acetate: n-hexane (2:3) as a mobile phase. Then, the product obtained was filtered and washed with ethanol. The precipitate was then dried over silica gel until fully dried. For precursor **2a**, it was accomplished via Williamson ether reaction using 4-acetamidophenol (0.018 mole, 3g), 1-bromohexane (0.018 mole, 2.5g) and potassium carbonate (0.018 mole, 2.5g). The reaction resulted in a white precipitate and a colorless solution. TLC technique was used to determine the completion of the reaction. After cooling to room temperature and vacuum removal of the solvent, white solid was obtained. Then, the obtained white solid of **2a** was refluxed with constant stirring in a mixture of ethanol and concentrated acid for *ca.* 2 hours. This reaction has afforded **3a**, along with light brown solution. To obtain the **AZ** additive, the precursor of **1** (0.0018 mole, 0.5g) was fully dissolved in ethanol (100 mL) whilst, the precursor of **3a** (0.0018 mole, 0.35g) was completely dissolved in ethanol (30 mL) before being added dropwise to the precursor of **1**. Once both compounds were fully dissolved, reflux process was initiated. The reaction was refluxed for approximately 6 hours at 70 ℃, the boiling point of ethanol. When adjudged completion also via TLC, the orange precipitate obtained was filtered and collected. The overall chemical pathway for the synthesis of **AZ** additive is represented in Scheme 1.

Preparation of solid biopolymer electrolyte (SBE)

An amount of chitosan (2g) was dissolved in 2% acetic acid and stirred continously for 4 hours. The obtained **AZ** additive was dissolved in 1 mL acetic acid and added into chitosan solution until a clear solution was achieved. The composition of **AZ** additive (2 wt.% to 8 wt.%) were added into the chitosan solution to obtain new SBE (**F1** – **F4)** is presented in Table 1. The solution was then casted into glass petri dishes, followed by drying in an oven at 50℃ for 30 hours. In this work, a maximum amount of 8 wt. % was tested to form clear solution and film.

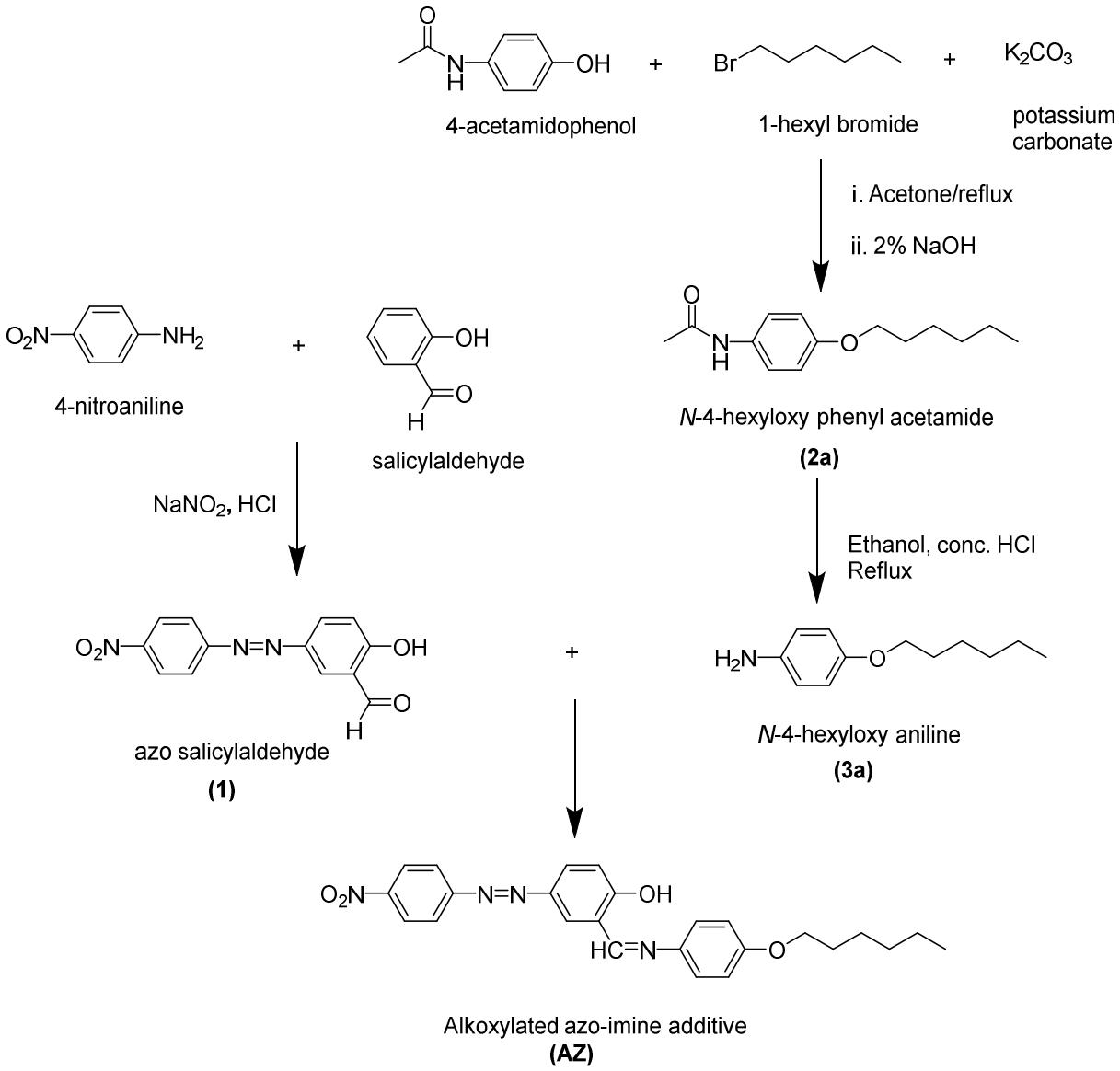

Scheme 1: Preparation of **AZ** additive

Table 1. Formulation of solid biopolymer electrolyte

Coding	Additive, wt.%	Weight percentage of additive, g	Chitosan, g
F0	0	0	2
F1	2	0.04	2
F2	4	0.08	2
F3	6	0.12	2
F4	8	0.16	2

Electrical impedance spectroscopy (EIS)

The prepared SBE was evaluated using EIS model HIOKI 3532-50 LCR Hi-Tester to determine its conductivity. For EIS measurement, 2 cm diameter of SBE was sandwiched between two stainless steel electrodes and tested in room temperature at a frequency range of 1 MHz to 50 Hz. The data was presented in the Cole-Cole plot form. The ionic conductivity, σ, of the electrolyte was calculated by using equation 1 [28] .

$$\sigma = \frac{t}{R_b \cdot A} \quad (1)$$

From eq. 1, t is the thickness of the electrolyte, R_b is the bulk resistivity and A is the (cm^2) electrode-electrolyte contact area. The value of R_b is retrieved from the Cole–Cole plot.

Results and Discussion

Spectroscopy technique

Figure 1 shows the IR spectra of precursors (**1**, **2a** & **3a**) and targeted compound of **AZ** additive. **AZ** additive revealed all the bands of interests namely ν(C-H), ν(C=N), ν(N=N), and ν(NO_2). The aliphatic C-H stretching vibrations arise at 2921 and 2856 cm^{-1} of the alkoxy substituent. The assignment of the stretching mode was made by comparison to their precursors **2a** and **3a** which indicates that the intensities of these bands increased. The absence of the stretching modes of residual amino, ν(NH_2) from precursor (**3a**) and aldehyde ν(CHO) groups from **1** together with the appearance of a typical band of imine bonds, ν(C=N) at 1614 cm^{-1} have provided strong evidence to the Schiff base formation reaction for **AZ** additive [29]. Two bands of ν(N=N) occur at 1500 cm^{-1} and 1440 cm^{-1} represent the asymmetric and symmetric N=N stretching vibrations of azo moiety [30, 31]. The shifting of ν(N=N) band to the higher wavenumber compared to **1** is due to the enhanced of mesomeric and inductive effect of the substituents. The characteristics of nitro group shifted to a slightly lower wavenumber at 1343 cm^{-1} due to stretching vibrations of ν(NO_2).

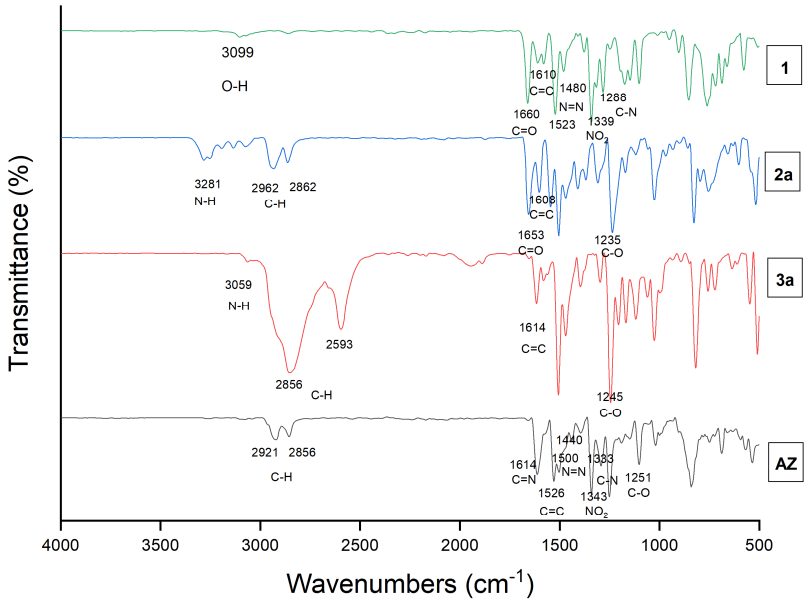

Figure 1. IR spectra of precursors and **AZ** additive

From Figure 2, the ^1H NMR spectrum for **AZ** additive reveals the methyl protons at δ_H 0.92 ppm while protons for methylene group were detected in the region of δ_H 1.35-1.82 ppm. The signal of R-O-CH_2 deshielded at δ_H 4.00 ppm due to the contribution of electronegativity of the oxygen atom. The closer the proton

approaches the electronegative oxygen atom, the greater the deshielding effect and therefore the resonance of R-O-CH_2 shifted towards downfield as compared to CH_3 which is located further from the oxygen atom. The values are in good agreement with the previous literature reported by Nakum and team [32]. The resonance of aromatic protons of *para*-substituted aromatic ring can be clearly observed as a pseudo-doublet resonance in the range of δ_H 6.82 ppm − 6.98 ppm and δ_H 7.66 ppm − 7.82 ppm and is considerably downfield due to large anistropic effect. The CH=N and hydroxyl protons found at around δ_H 8.06 ppm and δ_H 8.71 ppm respectively, are characterized by their unique singlet resonance at downfield [33], thus confirming the targeted compound.

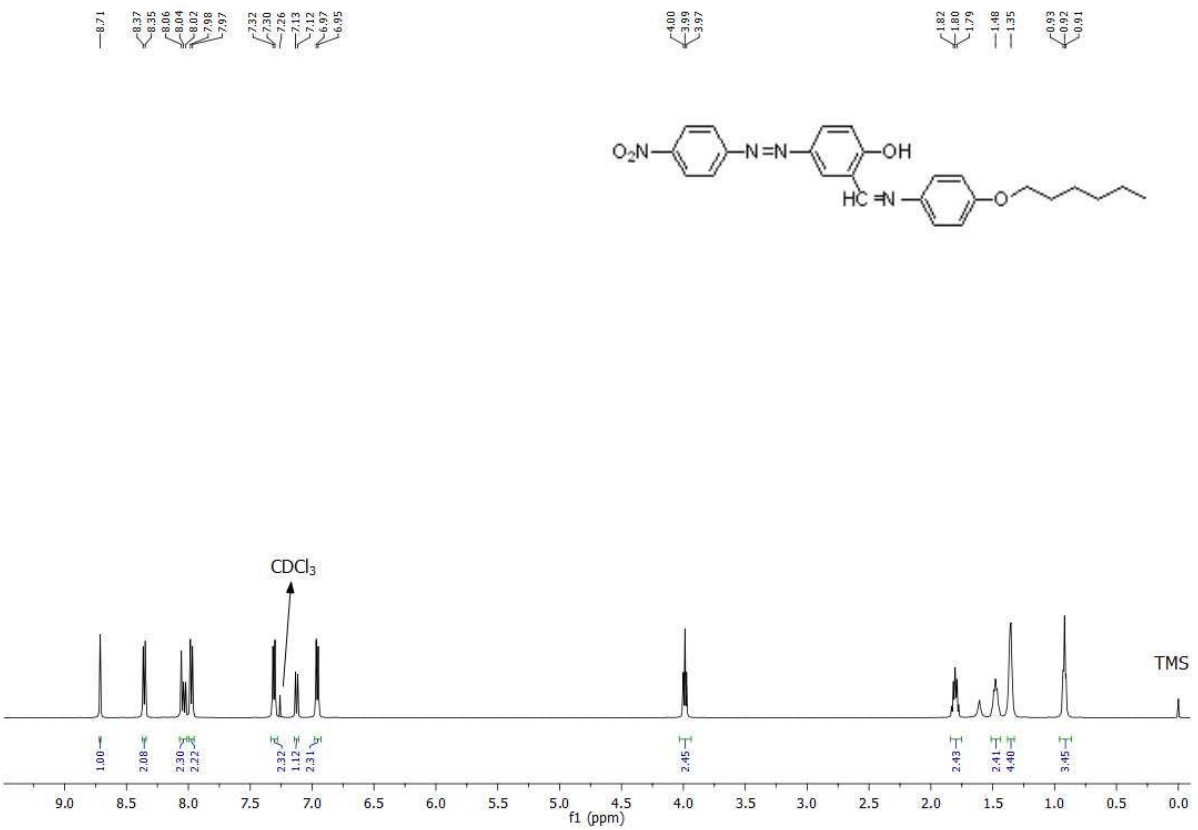

Figure 2. ^{1}H NMR for the **AZ** additive

Based on ^{13}C NMR spectrum of **AZ** additive, all expected resonances are at appropriate and expected chemical shifts. The carbon resonance of the terminal methyl group (CH_3) appears around δ_C 14.03 ppm, while for alkyl chain length, it appeared in the range of δ_C 22.60-35.57 ppm. The chemical shift for R–CH_2-O- can be found at δ_C 62.69 ppm due to the deshielding effect and is similar to Nakum et al. [34]. The resonances of aromatic ring carbon were assigned in the range of δ_C 115.29-155.85 ppm. The signal observed at δ_C 165.57 ppm is attributed to the C=N carbon atom which indicates the presence of imino linkage in the **AZ** additive.

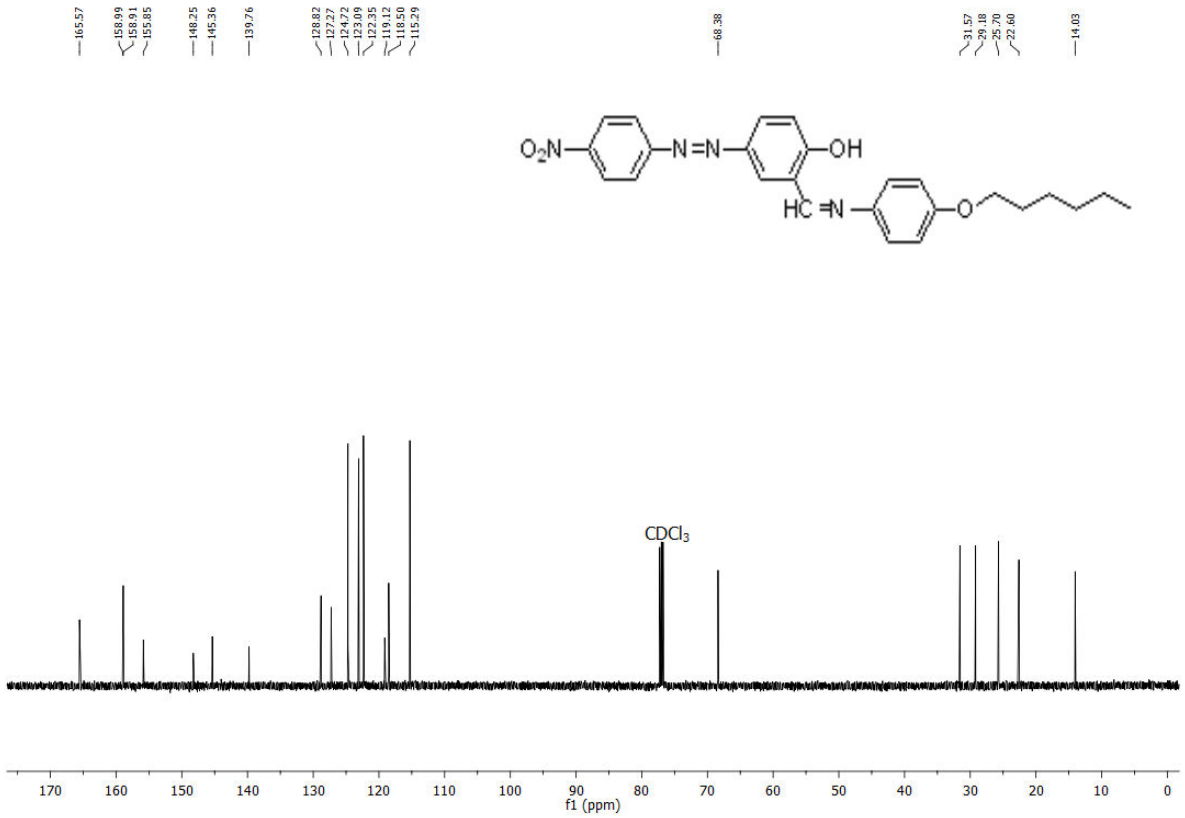

Figure 3: ^{13}C spectrum of the **AZ** additive

Thermogravimetric analysis (TGA)

TGA of precursors (**1**, **2a**, and **3a**) and **AZ** additive were carried out to investigate their thermal property. Based on the thermograms shown in Figure 4, no weight loss was observed at temperature below 120 °C. This indicated absence of water or solvent molecules that are left or trapped during the synthetic reaction and recrystallization. All synthesized compounds exhibited only one step of thermal degradation with different onset and offset values. By comparing the onset temperature of each compound, **AZ** additive was found to be stable up to 300 °C indicating that it has higher thermal stability compared to its precursor and therefore chosen as the additive to be tested in this study. The degradation of **AZ** additive was not complete at 600 °C, with 42.55% of residue left. This value coincides with the reported value by Ahmed et al. [35]. This may be due to the degradation of azo moiety which occurred through the cleavage of the azo bond by reductive process as suggested by previous studies [35, 36]. The trend of the thermal stability can be clearly observed by the presence of azo and alkoxy group in **AZ** additive. Ultimately, it can be concluded that the stability of additive increases as the degradation increases and it also depends on the substituent and molecular weight of the material. The thermal degradation parameters are given in Table 2.

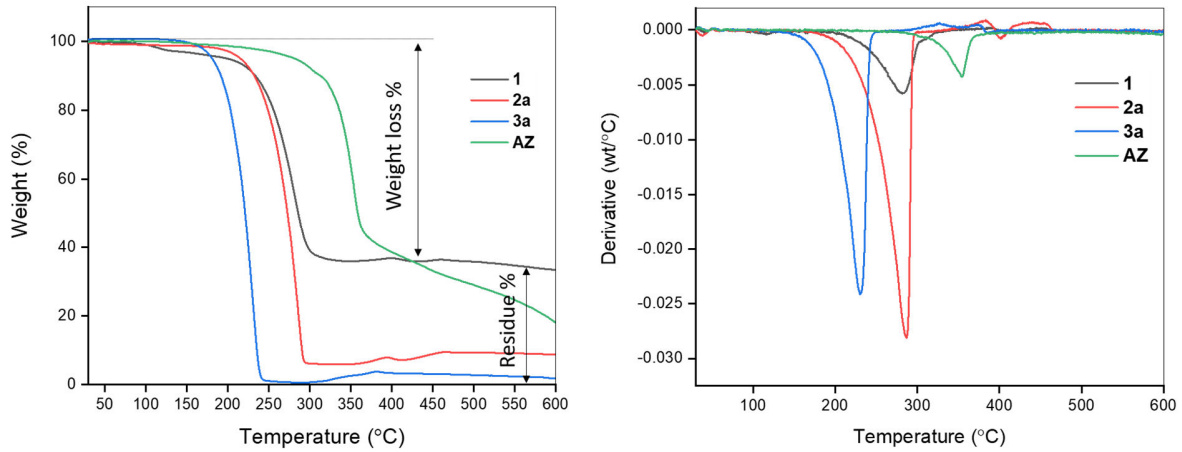

Figure 4. TGA and DTG of precursors and **AZ** additive

Table 2. Thermal degradation parameters of precursors and **AZ** additive

Compound	**T_{onset} (°C)**	**T_{max} (°C)**	**Weight Loss (%)**	**Residue (%)**
1	243	300	62.91	37.09
2a	254	289	92.6	7.4
3a	204	235	99.83	0.17
AZ additive	319	348	57.45	42.55

Ionic conductivity analysis

Impedance spectroscopy is typically used to study the electrical properties of the electrolytes. The Cole-Cole plot for the prepared SBE system is illustrated in Figure 5. From the plots, chitosan-based solid biopolymer electrolyte shows high-frequency region semicircle arc and low-frequency region inclination spike, where both are related to ionic conduction in the bulk of sample. Upon the addition of additives, the semicircle of chitosan disappeared and bulk resistance (R_b) decreases. The SBE with the incorporation of 4% additive (**F2**) gives the highest ionic conductivity value of 8.22 x 10^{-3} S/cm.

Figure 6 shows the ionic conductivity of the prepared SBE. The ionic conductivity value for chitosan SBE (without addition of additive) is 7.38 x 10^{-10} S/cm which is comparable with reported results by Rahman et al. [13]. The value shows the significant trends where it shows the increment of values upon the addition of **AZ** additive in the polymer host matrix of up to 8.22 x 10^{-3} S/cm for SBE containing 4 wt.% **AZ** additives. The increment in ionic conductivity can be attributed to the enhancement in the number density of charge carriers and efficiency of synthesized additives in dissociating chitosan matrix [37]. However, the value decreases after 6 wt.% because it has already reached the optimum concentration, thus leading towards sample aggregation [11]. From the preliminary result, **AZ** additive reveals good potential as an additive agent in SBEs as it can improve the ionic conductivity of the system with a potential in electrolyte application.

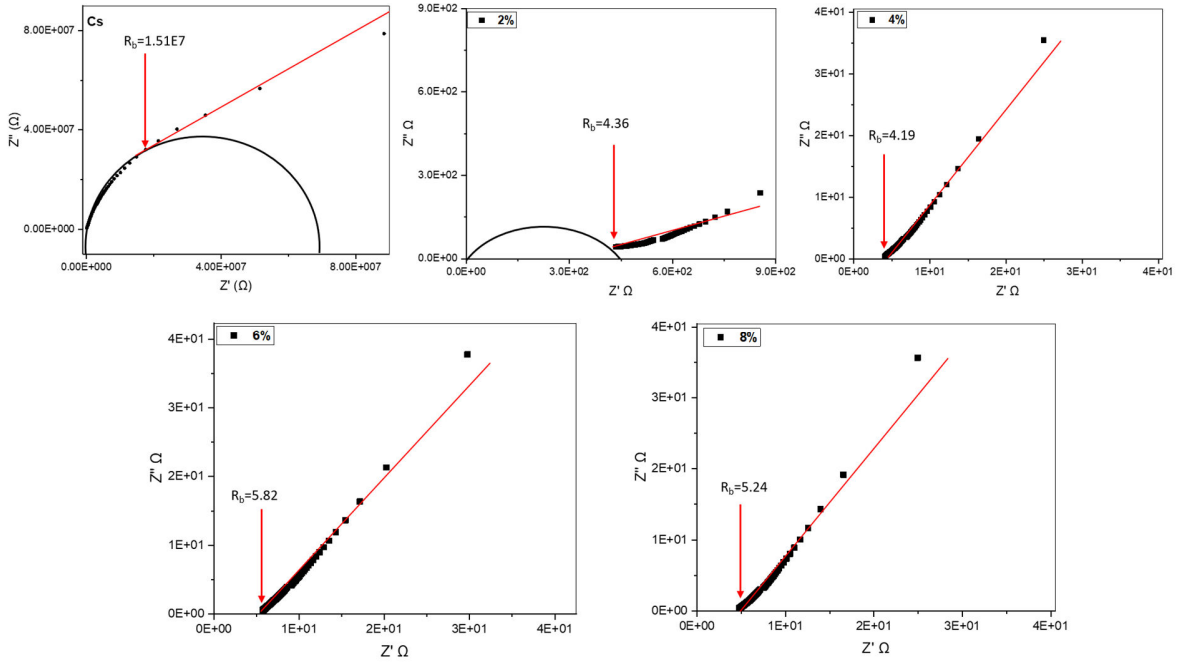

Figure 5. Cole-Cole plot of chitosan and variation weight percent of additive

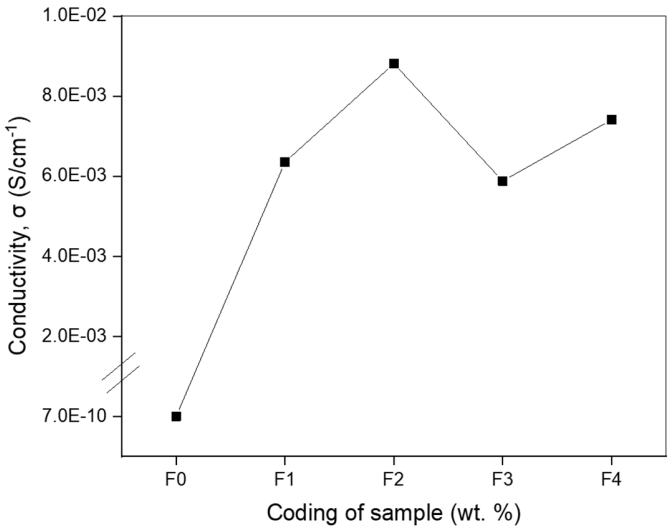

Figure 6. Conductivity of SBE system

Conclusion

This present work has successfully introduced a new **AZ** additive material integrated into chitosan biopolymer electrolyte to enhance charge carrier mobility and conductivity performance. All synthesized compounds including the precursors and **AZ** were analyzed via FTIR, 1D NMR, and TGA. TGA studies show that the effect of **AZ** influenced the thermal stability of the SBEs system by increasing the temperature decomposition (T_d) and is stable up to 300 °C. The ionic conductivity of the prepared SBEs system have been successfully evaluated using EIS and shows an increment in the order of 10^{-7} S/cm to 10^{-3} S/cm with the addition of **AZ** additive.

The maximum conductivity at ambient temperature (303 K) achieved up to 8.22 x 10^{-3} S/cm at 4% of additive. The preliminary finding reveals that the presence of active group of hydroxyl (-OH) and azo (N=N) can significantly affect the conductivity performance. Hence, the output from this work creates an alternative approach to initiate further investigation on new, efficient, stable additive materials in various optoelectronic application.

Acknowledgement

We would like to acknowledge the research grant support from Ministry of Higher Education, Malaysia for Fundamental Research Grant Scheme, FRGS/1/2021/STG05/UNIMAP/03/1 (9003-00914) and Faculty of Chemical engineering & Technology, Universiti Malaysia Perlis for facilities and research aids.

References

1. Li, X., Ding, C., Li, X., Yang, H., Liu, S., Wang, X., Zhang, L., Sun, Q., Liu, X. and Chen, J. (2020). Electronic biopolymers: From molecular engineering to functional devices. *Chemical Engineering Journal,* 397: 125499.
2. Mirzaeian, M., Abbas, Q., Ogwu, A., Hall, P., Goldin, M., Mirzaeian, M., and Jirandehi, H. F. (2017). Electrode and electrolyte materials for electrochemical capacitors. *International Journal of Hydrogen Energy,* 42(40): 25565-25587.
3. Pan, Q., Gong, D., and Tang, Y. (2020). Recent progress and perspective on electrolytes for sodium/potassium-based devices. *Energy Storage Materials*, 31: 328-343.
4. Hakari, T., Yoshimi, S., Nagao, K., Sakuda, A., Tatsumisago, M., and Hayashi, A. (2022). Thermally stable bulk-type all-solid-state capacitor with a highly deformable oxide solid electrolyte. J*ournal of Power Sources,* 543: 231821.
5. Zeng, Q., Lv, Z., Li, S., Yang, B., He, J., and Song, J. (2023). Electrolytes for liquid metal batteries. *Materials Research Bulletin,* 2023: 112586.
6. Sun, J., Yuan, H., Yang, J., Zhang, Y. W., and Wang, J. (2023). Electrolytes for better and safer batteries: Liquid, solid or frameworked, what's next?. *Next Materials,* 1(3): 100024.
7. Taneja, N., Kumar, A., Gupta, P., Gupta, M., Singh, P., Agrawal, N., Bocchetta, P. and Kumar, Y. (2022). Advancements in liquid and solid electrolytes for their utilization in electrochemical systems. *Journal of Energy Storage,* 56: 105950.
8. Varshney, P. K., and Gupta, S. (2011). Natural polymer-based electrolytes for electrochemical devices: a review. *Ionics,* 17(6): 479-483.
9. Yusuf, S. N. F., Yusof, S. Z., Kufian, M. Z., and Teo, L. P. (2019). Preparation and electrical characterization of polymer electrolytes: A review. *Materials Today: Proceedings,* 17: 446-458.
10. Abdulwahid, R. T., Aziz, S. B., and Kadir, M. F. (2023). Environmentally friendly plasticized electrolyte based on chitosan (CS): Potato starch (PS) polymers for EDLC application: Steps toward the greener energy storage devices derived from biopolymers. *Journal of Energy Storage,* 67: 107636.
11. Khairul, W. M., Rahamathullah, R., Joni, J. R., and Isa, M. I. N. (2022). Density functional theory (DFT) calculations, synthesis and electronic properties of alkoxylated-chalcone additive in enhancing the performance of CMC-based solid biopolymer electrolyte. *International Journal of Hydrogen Energy,* 47(65): 27866-27876.
12. El-Hefian, E. A., Nasef, M. M., and Yahaya, A. H. (2014). Chitosan-based polymer blends: Current status and applications. *Journal of the Chemical Society of Pakistan,* 36(1): 11-27.
13. Rahman, N. A., Hanifah, S. A., Mobarak, N. N., Ahmad, A., Ludin, N. A., Bella, F., and Su'ait, M. S. (2021). Chitosan as a paradigm for biopolymer electrolytes in solid-state dye-sensitised solar cells. *Polymer,* 230: 124092.
14. Shaari, N., and Kamarudin, S. K. (2019). Recent advances in additive-enhanced polymer electrolyte membrane properties in fuel cell applications: An overview. *International Journal of Energy Research*, 43(7): 2756-2794.
15. Kumar, S., Dhapola, P. S., Pandey, S. P., Singh, P. K., and Chauhan, M. (2021). Corn-starch based porous carbon and IL based electrolyte for high efficient supercapacitor. *Materials Today: Proceedings,* 34: 842-845.
16. Aziz, S.B., Nofal, M.M., Abdulwahid, R.T., Kadir,

M.F.Z., Hadi, J.M., Hessien, M.M., Kareem, W.O., Dannoun, E.M. and Saeed, S.R. (2021). Impedance, FTIR and transport properties of plasticized proton conducting biopolymer electrolyte based on chitosan for electrochemical device application. *Results in Physics,* 29: 104770.

17. Perumal, P., and Selvin, P. C. (2021). Boosting the performance of electric double layer capacitor via engaging pectin macromolecular electrolyte with elevated ionic conductivity and potential window stability. *Chemical Engineering Journal Advances,* 8: 100178.
18. Marturano, V., Cerruti, P., and Ambrogi, V. (2017). Polymer additives. *Physical Sciences Reviews,* 2(6): 20160130.
19. Baran, T., and Menteş, A. (2016). Polymeric material prepared from Schiff base based on O-carboxymethyl chitosan and its Cu (II) and Pd (II) complexes. *Journal of Molecular Structure,* 1115: 220-227.
20. Shanavas, A., Vanjinathan, M., Nasar, A. S., Amudha, S., and Suthanthiraraj, S. A. (2012). Synthesis, thermal and solar cell application of novel hyperbranched polyurethanes containing azomethine and aryl-ether connectivities. *High Performance Polymers,* 24(7): 561-570.
21. Rahamathullah, R., Low, J. K., Khairul, W. M., Osman, R. A. M., and Isa, M. I. N. (2023). Fused aromatic disubstituted azomethine as organic additives in NH_4SCN doped CMC based electrolyte film. In AIP Conference Proceedings (Vol. 2703, No. 1). AIP Publishing.
22. Sarswat, P. K., Sathyapalan, A., Zhu, Y., and Free, M. L. (2013). Design, synthesis, and characterization of TPA-thiophene-based amide or imine functionalized molecule for potential optoelectronic devices. *Journal of Theoretical and Applied Physics*, 7: 1-9.
23. Kamali, S., Orojloo, M., Arabahmadi, R., and Amani, S. (2022). Design and synthesis of a novel azo-Schiff base ligand: Its application as a colorimetric chemosensor for selective detection of Ni^{2+} and CN^{-} in aqueous-organic media, computational studies, antimicrobial properties, and molecular logic circuits. *Journal of Photochemistry and Photobiology A: Chemistry,* 433: 114136.
24. Liu, M., Yin, L., Wang, L., Miao, T., Cheng, X., Wang, Y., Zhang, W. and Zhu, X. (2019). Synthesis of monodisperse aromatic azo oligomers toward gaining new insight into the isomerization of π-conjugated azo systems. *Polymer Chemistry,* 10(14): 1806-1811.
25. Rahamathullah, R., and Khairul, W. M. (2017). Evaluation on the electrochemically deposited alkoxy thiourea as liquid crystalline semiconductor film. *Applied Surface Science,* 424: 45-51.
26. Menati, S., Azadbakht, A., Azadbakht, R., Taeb, A., and Kakanejadifard, A. (2013). Synthesis, characterization, and electrochemical study of some novel, azo-containing Schiff bases and their Ni(II) complexes. *Dyes and pigments,* 98(3): 499-506.
27. Ma, I. W., Ammar, S., Bashir, S., Selvaraj, M., Assiri, M. A., Ramesh, K., and Ramesh, S. (2020). Preparation of hybrid chitosan/silica composites via ionotropic gelation and its electrochemical impedance studies. *Progress in Organic Coatings,* 145: 105679.
28. Kotatha, D., Torii, Y., Shinomiya, K., Ogino, M., Uchida, S., Ishikawa, M., Furuike, T. and Tamura, H. (2019). Preparation of thin-film electrolyte from chitosan-containing ionic liquid for application to electric double-layer capacitors. *International Journal of Biological Macromolecules,* 124: 1274-1280.
29. Purtas, F. Sayin,K. Ceyhan, G., Kose, M. and Kurtoglu, M. (2017). New fluorescent azo-Schiff base Cu(II) and Zn(II) metal chelates, spectral, structural, electrochemical, photoluminescence and computational studies. *Journal Molecular Structure,* 1137: 461-475.
30. Eskikanbur, S., Sayin, K., Kose, M., Zengin, H., McKee, V., and Kurtoglu, M. (2015). Synthesis of two new azo-azomethines; spectral characterization, crystal structures, computational and fluorescence studies. *Journal of Molecular Structure,* 1094: 183-194.
31. Gür, M., Kocaokutgen, H., Kandemirli, F., Özkinali, S., and Yerlikaya, Z. (2016). Synthesis, spectral and thermal characterization of some azo-polymers containing acrylate derivatives. *Research & Reviews: Journal of Chemistry,* 5(2):1-9.

32. Nakum, K. J., Katariya, K. D., Savani, C. J., and Jadeja, R. N. (2022). The influence of molecular flexibility on the mesogenic behavior of a new homologous series based on azo-azomethine: Synthesis, characterization, photoisomerization and DFT study. *Journal of Molecular Structure,* 1249: 131586.
33. Ozkinali, S., Cavus, M. S., and Sakin, B. (2018). Synthesis, structural characterization and theoretical investigations of new azo-azomethine compounds bearing acryloyl moiety. *Hittite Journal of Science and Engineering,* 5(4): 259-269.
34. Nakum, K. J., Katariya, K. D., Hagar, M., and Jadeja, R. N. (2022). The influence of lateral hydroxyl group and molecular flexibility on the mesogenic behaviour of a new homologous series based on thiophene-chalcone: Synthesis, characterization, crystal structure and DFT study. *Journal of Molecular Structure,* 1261: 132891.
35. Ahmed, N. H., Saad, G. R., Ahmed, H. A., and Hagar, M. (2020). New wide-stability four-ring azo/ester/Schiff base liquid crystals: Synthesis, mesomorphic, photophysical, and DFT approaches. *RSC Advances,* 10(16): 9643-9656.
36. Mali, H., Sharma, V. S., Rathod, S. L., Sharma, A. S., Shrivastav, P. S., and Prajapati, H. R. (2023). Synthesis, characterization and photophysical study of cholesterol functionalized azo-based room temperature liquid crystals. *Journal of Molecular Structure,* 1289: 135776.
37. Ismail, N. I., Saidin, S. N., RA, N. H., Ahmad, A., and NaiiM, N. (2022). The Effects of monosaccharides on the physico-electrochemical properties of chitosan based solid polymer electrolytes (SPEs). *Sains Malaysiana*, 51(8): 2461-2472.